

Studies of Biaxial Mechanical Properties and Nonlinear Finite Element Modeling of Skin

Xituan Shang*, Michael R. T. Yen^{1,†}, M. Waleed Gaber[‡]

Abstract: The objective of this research is to conduct mechanical property studies of skin from two individual but potentially connected aspects. One is to determine the mechanical properties of the skin experimentally by biaxial tests, and the other is to use the finite element method to model the skin properties. Dynamic biaxial tests were performed on 16 pieces of abdominal skin specimen from rats. Typical biaxial stress-strain responses show that skin possesses anisotropy, non-linearity and hysteresis. To describe the stress-strain relationship in forms of strain energy function, the material constants of each specimen were obtained and the results show a high correlation between theory and experiments. Based on the experimental results, a finite element model of skin was built to model the skin's special properties including anisotropy and nonlinearity. This model was based on Arruda and Boyce's eight-chain model and Bischoff et al.'s finite element model of skin. The simulation results show that the isotropic, nonlinear eight-chain model could predict the skin's anisotropic and nonlinear responses to biaxial loading by the presence of an anisotropic prestress state.

Keyword: Skin, Biaxial Mechanical Properties, Finite Element Modeling

1 Introduction

The mechanical properties of skin are important indicators of the skin's pathological situations and wound healings. The mechanical properties of skin have been widely applied in the diagnosis of certain diseases, in the design of plastic surgeries and in the development of artificial skin. Understanding the cause of conditions like this requires detailed knowledge of the structural-mechanical properties of the normal skin, so that the abnormalities can be identified.

The skin's mechanical properties have been intensively studied and there are many different approaches to define the skin's mechanical properties (Wilkes, Brown, & Wildnauer 1973; Thacker, Lachetta, Allaire, Edgerton, Rodeheaver, & Edlich 1977; Larrabee 1986; Hildebrandt, Fukaya, & Martin 1969; Lanir, & Fung 1974; Ridge, & Wright 1966; Gibson, Stark, & Evans 1969; Alexander, & Cook 1977; Ohura, Singihara, & Honda 1980; Clark, Cheng, & Leung 1996; Grahame, 1969; Kirk, & Chieffi 1962; Gambarotta, Massabo, Morbiducci, Raposio, & Santi 2005; Schneider, Davidson, & Nahum 1984; Wan Abas 1994). These research approaches can be categorized according to the type of load action applied to the skin, i.e., uniaxial and biaxial extension, suction, indentation and torsion loading. These methods yield the force-deformation relation, which can be converted into the stress-strain relationship for the derivation of the constitutive equation (Tong, & Fung 1976).

Though uniaxial tests are the most widely used method in skin researches, they can not exactly define the mechanical properties of a three-dimensional solid material, such as skin. More specifically, the constitutive equations that characterize soft tissues in three dimensions can not be

* Department of Biomedical Engineering, The University of Memphis, Memphis, TN 38152.

† Corresponding Author. Department of Biomedical Engineering, ET-330, The University of Memphis, Memphis, TN 38152. Email: myen@memphis.edu, Tel: 901-678-3263.

‡ Department of Biomedical Engineering, The University of Tennessee, Health Science Center at Memphis, TN 38163.

generalized from one-dimensional data (Lanir, & Fung 1974). A comprehensive three-dimensional model of the skin can be constructed only on the basis of three-dimensional tests. It is generally accepted in the literature that for incompressible solid material, any change in the third dimension can be calculated from the changes in the other two dimensions. Therefore a complete three-dimensional model could be determined from two-dimensional tests (Lanir, & Fung 1974). Fortunately, the skin can be regarded as incompressible materials, so two-dimensional tests of the skin data could be used to yield a three-dimensional stress-strain relationship model.

The first investigators who developed and utilized *in vitro* biaxial testing of skin were Lanir and Fung (1974). They tested abdominal skin specimens from 47 albino male rabbits under different test protocols. The tests they carried include the biaxial and uniaxial slow-rate-of-stretching tests; and biaxial and uniaxial relaxation tests after quick stretching. They also tested the effect of temperature on biaxial relaxation tests.

Their experimental results show that: (1) Skin's stress-strain relations are extremely nonlinear. Hysteresis was observed at all strain rates, but the loading and un-loading stress-strain responses are independent of the strain rate. (2) The skin is anisotropic in its mechanical properties and the material axis depends on the specimen's anatomic orientation, but probably possesses orthotropic symmetry. (3) The relaxation curve does not terminate at the origin and returns to it only after a long period of relaxations. (4) A comparison of uniaxial and biaxial stretch tests on the same specimen shows that for a given stretch ratio in the loading direction, the stress with the uniaxial test is considerably lower than that in the biaxial condition. (5) The temperature effect on the mechanical properties depends both on the rate of temperature change and on the strains and stress of the tissue. (Lanir, & Fung 1974).

In this research, dynamic biaxial tests were performed on 16 pieces of abdominal skin specimen from rats using the biaxial test experimental system EHMI BIAX-II. First we will have a brief introduction about the experimental system.

2 Introduction of Biaxial Test Experimental System

The biaxial testing equipment EHMI BIAX-II was custom-designed at the University of California at San Diego in 1999. This system was designed to test the sheet-like soft tissues biaxially. Figure 1 is the picture of the equipment. The main components of the equipment are: (1) the loading frame, (2) computer I and amplifier controller unit, (3) camera mount and video camera. Two additional pieces of equipment, a video dimensional analyzer (VDA) and computer II were used to process the video signal to measure the strains in two orthogonal directions. (Gao, Huang, & Yen 1998).



Figure 1: Experimental equipment overview

2.1 Stretching Mechanism

As shown in Figure 2, the specimen floats in physiological saline solution contained in an open-to-atmosphere compartment. Each edge of the specimen was hooked by small staples to 6 or 8 silk threads, which were connected to four platforms and loading mechanism. This set up allows individual adjustment of the tension of each thread.

The BIAX-II equipment is displacement (strain) controlled and records force. Displacement is controlled by programming a number of steps in the stepper-motor, which turns the lead screw and moves the actuator in or out. Each step is 1/10000" (2/10000" for two actuators) and the maximum speed is 50 mm/sec.

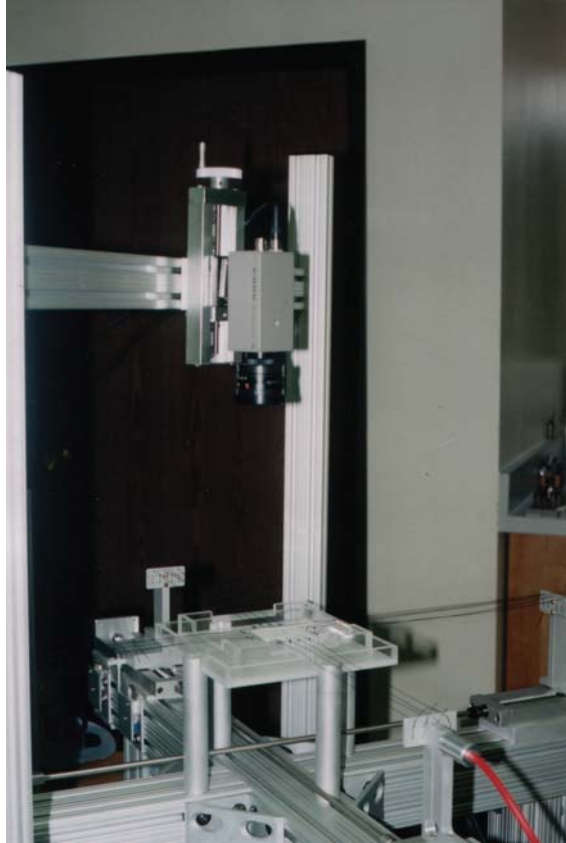


Figure 2: Setup of the specimen hooking

2.2 Non-contact Strain Measurement

The non-contact measurements of the strains are fulfilled by the VDA, video camera and computer II with image acquisition card and image analysis software.

In BIAX-II system, the VDA is used to acquire the deformation of the specimen in the y direction. The VDA keeps track of the movement of the parallel markers placed on top of the specimen and outputs the distance between them simultaneously. The advantage of using VDA is that it allows for non-contacting, real-time displacement measurements.

The BIAX-II system was not equipped with a second video camera and VDA, which may have involved complications in the setup with the first one. Therefore, additional setup was needed to track the deformation in the x direction. By using another computer with image acquisition card (ATI TV wonder, ATI Technologies Inc.) and

video capture software (Video Capturix, Capturix Technologies Inc., Portugal), the video signal can be automatically grabbed and extracted from the VCR at up to 30 frames /sec. Then the grabbed images can be analyzed with the image processing software named Scion Image.

Strain channels were calibrated using a set of reference rulers ranging from 3 mm to 30 mm. The goodness of fit (R) for the VDA channel was 0.9996 ± 0.0003 . The other channel has an error of 2%.

2.3 Force Measurement

The BIAX-II system picks up three channels of signals, including the force x , force y and the video camera signal. The force in each direction was measured by a force transducer attached to one of the platforms, and controlled through a feedback circuit. The force transducer reads between 0~1000 g weight full scales.

Both force channels were calibrated using a set of reference weights ranging from 1 g weight to 1000 g weight. The goodness of fit (R) in these force channels are

0.9997 ± 0.0002 and 0.9993 ± 0.0003 , respectively. The sampling rate of experimental data is set to 100 Hz. Such a treatment has ensured the accuracy of the collection of the stress and strain information.

3 Biaxial Experimental Protocols & Results

3.1 Specimen Preparation

Sixteen Sprague-Dawley adult male rats weighing 300 ± 20 g were used in the study. The rats were sacrificed and thoroughly shaved in the abdominal area. A square specimen of 50 mm by 50 mm was cut out, two boundaries were parallel to the body length direction and two boundaries were normal to it. The dimensions and the thickness of the skin were measured. Then the specimen was put into the open compartment of the BIAX-II equipment filled with saline solution. Each edge of the specimen was hooked using 8 small staples connected to the platform through nylon sutures (as illustrated in Figure 2). To minimize the effects of swelling of the specimen, the specimen stayed

in the saline solution at room temperature for at least 4 hours before performing the test (Lanir, & Fung 1974).

3.2 Strain Measurement

A square target (about 10 mm by 10 mm) was made on the center of each specimen by means of four wire markers made from 200 μ m diameter steel wires. The 10 mm long wires were bent in the middle at a right angle to L shape. One leg of the wire was pressed into the surface, while the other was laid on top of it. As shown in Figure 3, four steel wires were shown as white lines in the dark background of the specimen. The frame was used as a target to measure the strains.

Because the target area occupied only a small central portion of the specimen, the edge effects caused by staples were minimized (Lanir, & Fung 1974). If the shape of the rectangular did not change during the course of the experiment, the stresses and strains in the target area were regarded as uniformly distributed (Lanir, & Fung 1974; Nielsen, Hunter, & Smaill 1991).

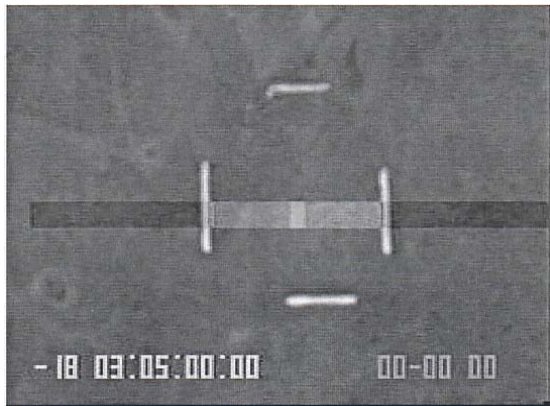


Figure 3: Overview of the specimen on the image monitor

3.3 Dynamic Test Procedures

It's found that the biaxial tests require biaxial preconditioning to get a repeatable and predictable stress-strain relationship (Lanir, & Fung 1974). In this case, the specimen was cycled according to

each test protocol about 10~12 times until a repeatable force-displacement curve is observed.

Two types of constant low stretch rate (1 mm/sec) biaxial tests protocols were performed in this study: (1) Step test: the strain in one direction is kept constant in each run but varied in 4 or 5 successive runs; in the other direction, the specimen was cycled from the preload to the maximum load and back to the preload. (2) Ramp test: both directions are simultaneously cycled from the preload to the maximum load and back to the preload in a triangular form. The ramp test is also called the equi-biaxial deformation test in the literature. The stepper-motor, which controls the stretching, moves at a speed of 1 mm/sec.

3.4 Constitutive Equation of Skin Elasticity

From the point of view of biomechanics, the properties of a tissue are known if its constitutive equation is known (Tong, & Fung 1976). The constitutive equation is the equation describing the stress-strain relationship of a material under a general three-dimensional stress field.

Many various forms of nonlinear strain-energy functions have been proposed for planar soft tissues. Some of them assume the material is isotropic (Nielsen, Hunter, & Smaill 1991), or orthotropic (Fung 1993; Tong, & Fung 1976; Demiray, & Vito 1976; Shoemaker, Schneider, Lee, & Fung 1986), and some of models are structural constitutive model (Arruda, & Boyce 1993; Lanir 1994; Bischoff, Arruda, & Grosh 2004). Almost all the experimental and modeling of soft tissue presented in the literature dealt only with quasi-static behaviors of the skin. Time dependent behaviors, such as viscoelasticity and poroelasticity, have not been examined in a biaxial stress-state, largely due to experimental technical limitations (Sacks 2000).

Among all these constitutive models, the model proposed by Tong and Fung (Tong, & Fung 1976) is the most widely used for planar soft tissues. The model was based on experimental data of rabbit abdominal skin collected by Lanir and Fung (Lanir, & Fung 1974). This model has been applied on the modeling of different soft tissues, including skin, pericardium, myocardium, visceral

pleura, artery, etc. (Sacks 2000).

Tong and Fung's model was used in this study. Following is the strain-energy function proposed by Tong and Fung:

$$\begin{aligned} & \rho_0 W^{(2)} \\ &= \frac{1}{2}(\alpha_1 E_1^2 + \alpha_2 E_2^2 + \alpha_3 E_{12}^2 + \alpha_3 E_{21}^2 + 2\alpha_4 E_1 E_2) \\ &+ \frac{1}{2}c \exp(a_1 E_1^2 + a_2 E_2^2 + a_3 E_{12}^2 + a_3 E_{21}^2 \\ &+ 2a_4 E_1 E_2 + \gamma_1 E_1^3 + \gamma_2 E_2^3 + \gamma_4 E_1^2 E_2 + \gamma_5 E_1 E_2^2) \end{aligned} \quad (1)$$

In the above equation, the first linear part accounts for the linear part in the stress-strain curve, and the exponential part accounts for the high-stress nonlinear region.

ρ_0 is the density of the material in the initial undeformed state. W is the strain energy per unit mass of the material, then $\rho_0 W$ is the strain energy per unit volume of the tissue in the zero stress state. α 's, a 's, γ 's and c are constants. E_1 and E_2 are Green's strains in the x and y direction, respectively, and E_{12} is the shear strain, which was kept zero in the experiments. We determined the constants based on the biaxial experimental results.

3.5 Experimental Results

Experimental data based on biaxial tests on 16 pieces of abdominal skin specimen from rats are presented. The specimens were tested according to various combinations of the test protocols. The head-to-tail direction is defined as the x direction and the transverse direction is defined as the y direction.

Some of the typical test results are shown in Figures 4 to 7. Typical stress-strain deformation response to biaxial loading and unloading is shown in Figure 4. Typical loading stress-strain curves with four step-fixed strains are shown in Figure 5. Typical equibiaxial loading stress-strain curves are shown in Figure 6. The comparison between the theoretical and experimental loading stress-strain curves in both directions for one specimen is shown in Figure 7.

Figure 4 presents the typical loading and unloading force-strain curves of a skin specimen sub-

jected to a varied stretch ratio in one direction and fixed stretch ratio in the transverse direction (stretch ratio in transverse direction is 1.00). The force in the direction of stretching is plotted against the stretch ratio. It is observed that the nonlinearity becomes evident as the stretch ratio exceeds 1.2. Skin shows anisotropic properties. Hysteresis was noted between the loading and unloading curves. In the following tests results, only the loading phase data were presented.

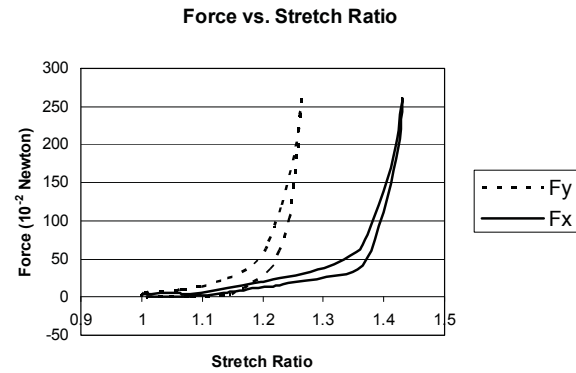


Figure 4: Loading and unloading force-strain curves of a skin specimen subjected to varied stretch ratios in one direction and fixed stretch ratio in the transverse direction (transverse stretch ratio is 1.00). The force in the direction of stretching is plotted against the stretch ratio.

Figure 5 presents typical loading stress-strain curves of a skin specimen subjected to four step-fixed stretch ratios (1.000 to 1.186 equally divided) in the x direction, and varied stretch ratios in the y direction. The upper figure is the Lagrangian stress T_{yy} plotted against the stretch ratio L_y in the biaxial loading process, and the lower figure is transverse stress T_{xx} vs. L_y . The numbers in parentheses are the corresponding standard deviations of L_x (sample size = 4). It is seen that as the step strain increases in the x direction, the stress-strain curves shift both left and upward. Again, the nonlinear characteristics appear evident as the strain increases.

Figure 6 presents the typical equibiaxial loading stress-strain curves for a specimen. The Lagrangian stresses in both directions are plotted against the strain $e = \frac{L_1 - L_0}{L_0}$.

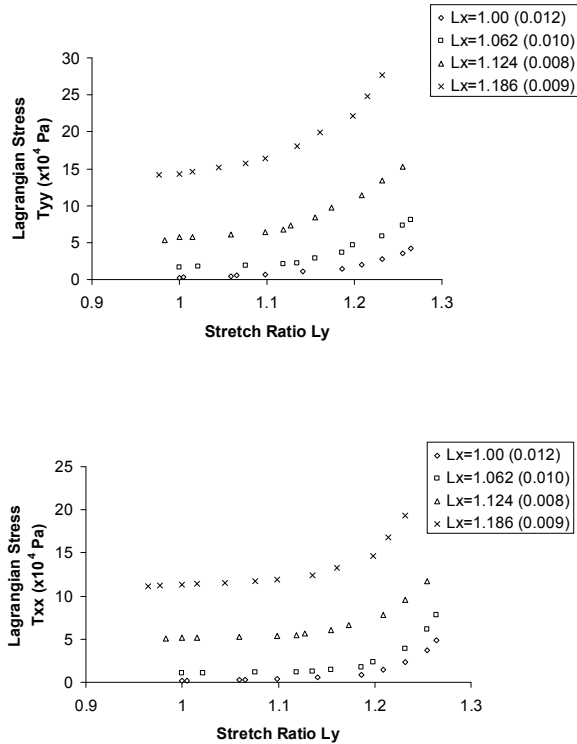


Figure 5: Typical loading stress-strain curves of a skin specimen subjected to four fixed strains in the x direction, and varied stretch ratios in the y direction. The upper figure is the Lagrangian stress T_{yy} plotted against the stretch ratio L_y in the biaxial loading process. The lower figure is transverse stress T_{xx} vs. L_y . The number in parentheses are the corresponding standard deviations of L_x (sample size = 4).

Two sets of experimental curves are used to determine the coefficients in the strain-energy function. One is the stress-strain relations with E_2 fixed and one with E_1 fixed. Curve fitting software NLREG and MATLAB program were used to determine the constants with the minimized sum of the square errors of these equations.

Based on the parameter estimation technique as described in the previous section, the values of the unknown constants $\alpha_1, \alpha_2, \alpha_4, a_1, a_2, a_4$ and c in the strain energy function can be obtained (Table 1). The material constants were calculated from 10 specimens. Figure 7 shows the comparison between the theoretical and experimental loading force-strain curves in both directions for a speci-

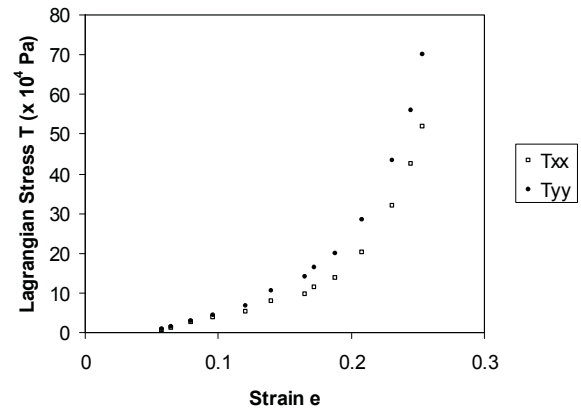


Figure 6: Typical equibiaxial loading stress-strain curves. The Lagrangian stresses in both directions are plotted against the nominal strain e .

men. Good agreement was observed.

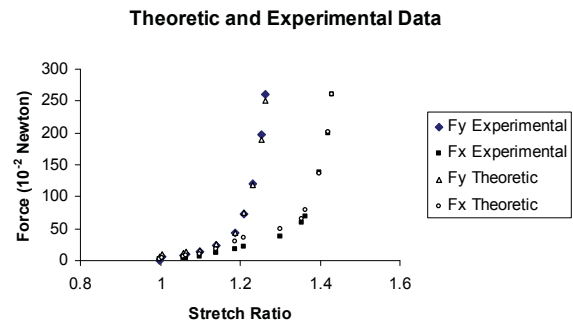


Figure 7: Comparison between the theoretical and experimental loading force-strain curves in both directions for a piece of specimen. Good agreement was observed.

4 Finite Element Modeling of Skin

4.1 Introduction

A successful finite element model of skin deformation under stretch can be used to determine the deformation of skin after the application of a specific force, to predict the force needed to for displacement of a point (wound closure) and to study the deformation of all points of the entire area based on the suture applied (Molinari, Fato, De Leo, Riccardo, & Beltrame 2005).

Orthopedic surgeons have been the primary clinicians interested in the finite element method

Table 1: The material constants of the strain-energy function

Constants	$\alpha_1 = \alpha_2(N/m^2)$	$\alpha_4(N/m^2)$	a_1	a_2	a_4	$c(N/m^2)$
Mean	9.72	2.90	6.59	9.12	4.77	0.0048
SD	3.77	1.75	2.89	4.71	5.09	0.0080

(Larrabee, & Galt 1986). Before surgery, surgeons need to make accurate planning of the “stretch-ability” of the skin. Physical modeling of skin is of great value in help with this kind of planning. For example, when planning the excision of an area of skin, the surgeon has to decide if the excised area can be closed by simply drawing the edges together, by making a complex series of flaps which utilize hyperextensibility in an adjacent area, or whether the only solution is to graft skin from another site (Molinari, Fato, De Leo, Riccardo, & Beltrame 2005). Currently this planning is based almost exclusively on purely anatomical and geometrical considerations. In other words, surgeons use a “paper model” based on geometry (Retel, Vescovo, Jacquet, Trivaudey, Varchon, & Burtheret 2001). This “paper model” does not provide the surgeons with objective and reliable mathematical data about the behaviors of skin under examination (Retel, Vescovo, Jacquet, Trivaudey, Varchon, & Burtheret 2001; Molinari, Fato, De Leo, Riccardo, & Beltrame 2005).

Currently many finite element (FE) models have been built to model the skin’s mechanical properties and some of these models have been applied in computer-aided plastic surgeries (Dehoff, & Key 1981; Larrabee, & Galt 1986; Spilker, de Almeida, & Donzelli 1992; Flynn, Peura, Grigg, & Hoffman 1998; Kirby, Wang, To, & Lampe 1998; Berkley, Weghorst, Gladstone, Raugi, Berg, & Ganter 1999; Bischoff, Arruda, & Grosh 2000; Yoshida, Tsutsumi, Mizunuma, & Yanai 2001; Retel, Vescovo, Jacquet, Trivaudey, Varchon, & Burtheret 2001; Hendriks, Brokken, Van Eemeren, Oomens, Baaijens, & Horsten 2003; Molinari, Fato, De Leo, Riccardo, & Beltrame 2005; Holberg, Schwenzer, & Rudzki-Janson 2005). But most of these models treat the skin as either an isotropic or a linear elastic material. Larrabee and Galt (Larrabee, & Galt 1986) were the first to use the finite element method to model the skin’s mechanical behaviors. They used sim-

ple linear stress-strain function to model skin and its subcutaneous layer under deformation. Kirby et al. (Kirby, Wang, TO, & Lampe 1998) proposed a three-dimensional finite element model of skin based on Larrabee and Galt’s work in pig model. Kirby and coworkers’ model incorporated linear elastic anisotropic material constants and the non-linearity of material constants was assumed to be minimal. Retel et al. (Retel, Vescovo, Jacquet, Trivaudey, Varchon, & Burtheret 2001) used an isotropic, non-linear model to model the wound closure of skin and compared their results with an isotropic and Hooke’s law elastic linear model. Lott-Crumpler and Chaudhry (Lott-Crumpler, & Chaudhry 2001) employed a linear stress-strain relationship and non-linear strain components for orthotropic human skin modeling and used this model to compute the optimal suturing patterns for a triangular wound.

Larrabee and Galt (Larrabee, & Galt 1986) had demonstrated that the practical strains of 10% to 20% occur in surgical practice. Strains of this magnitude suggest the need for a nonlinear modeling approach using the theory of finite deformations. As shown in our previous biaxial studies, skin is a highly non-linear, anisotropic soft tissue, thus a successful FE model of skin requires these special properties to be represented in the model.

The objective of this study is to model the skin’s non-linear and anisotropic properties using finite element method. The model simulations are based on the two dimensional testing data from *in vitro* experiments we did.

In our previous studies of the biaxial properties of the skin, Tong and Fung’s (Tong, & Fung 1976) constitutive model was used to fit the biaxial experimental results. However, Tong and Fung’s model is a phenomenological constitutive model and the parameters in it have no physical meanings linked to them, and it is unable to elucidate the underlying mechanism of tissue engineering

(Fung 1993). On the other hand, structure constitutive models, which attempt to integrate information on tissue composition and structure to avoid ambiguities in material characterization, will offer insight into the function, structure and mechanics of tissue components (Sacks 2000).

In 1993, Arruda and Boyce (Arruda, & Boyce 1993) proposed a three-dimensional structure constitutive model for large deformation of rubbery elastic material. This model is also called the eight-chain model. This structure constitutive model is an isotropic, nonlinear constitutive model and can be used to capture the large, three-dimensional stress-strain behaviors of rubbery elastic materials. By using this eight-chain model, Bischoff et al. (Bischoff, Arruda, & Grosh 2000) proposed a finite element model of skin to describe the skin's anisotropic, non-linear properties. They tested the model with data from several *in vitro* and *in vivo* uniaxial tests, and the results showed that the model can predict and fit the uniaxial tests results of both animal skin specimens and human skin specimens from several literatures.

The strain energy function used in the eight-chain model is:

$$W = nk\theta N \left(\frac{r_c}{Nl} \beta + \ln \frac{\beta}{\sinh \beta} \right) - \theta c' \quad (2)$$

The stress-stretch relations can be written in terms of the difference in two principal stresses:

$$\sigma_1 - \sigma_2 = \lambda_1 \frac{dW}{d\lambda_1} - \lambda_2 \frac{dW}{d\lambda_2} \quad (3)$$

In equation 2, n is the network molecular chain density, Boltzmann's constant $k = 1.3807 \times 10^{-23}$, absolute temperature $\theta = 298K$, N is the number of rigid links of length l in the fiber, $\beta = L^{-1}(r_c/Nl)$ (L^{-1} is the inverse Langevin function, the Langevin function is defined as $L(x) = \coth(x) - (1/x)$) and c' is a combination of constants.

Using the eight-chain model described above, Bischoff et al. (Bischoff, Arruda, & Grosh 2000) proposed a finite element model of skin to describe the skin's anisotropic, non-linear properties. There were two hypotheses made in

their model: the first one is that the eight-chain constitutive model based on the entropy change upon stretching of long chain molecules using physiological meaningful parameters to represent the collagen network in skin could accurately model the elastic behavior of skin. The second one is that anisotropic behavior of skin could be modeled using an initially isotropic constitutive law that develops anisotropy in the presence of an anisotropic stress state. Anisotropic prestresses result in different stress-free shape dimensions of the specimens, which could result in an anisotropic constitutive response (Birchoff, Arruda, & Grosh 2000).

The material parameters in Equation (2) were recast in terms of appropriate collagen network descriptors: n represents the collagen fiber density and is directly manifested as initial skin stiffness and N represents the free length of the collagen fibers and dominates large-stretch behavior (Birchoff, Arruda, & Grosh 2000).

In this study, Arruda and Boyce's structure model and Bischoff et al.'s finite element modeling method were used to model the skin's properties showed under biaxial tests.

4.2 Methods

The finite element analysis software used in this study is ABAQUS/CAE 6.4 (Abaqus Inc., 2004). ABAQUS is a commercially available finite element analysis software package and is widely used in academic and industrial finite element modeling researches.

A two-dimensional continuum solid material and four-node linear, plane stress element CPS4 were used in the simulations. The relaxed dimension of skin tissue was assumed as 44 mm by 44 mm. The thickness was assumed as 1 mm. A homogeneous, solid section is defined and assigned to the models.

Because the specimen domain has two planes of symmetry, to save the computation time, only one quarter of the 44 × 44 mm domain is required discretization. In this quarter, 4356 (66 × 66) equally sized four-node elements were used. Force data were converted to nominal stress by di-

viding the force by the initial cross-sectional area used in the simulation.

The boundary conditions can be defined as follows: the nodes belonging to the two normal centered axes of the $44 \times 44 \text{ mm}$ domain must stay on those axes, and can be moved along those axes but cannot be moved perpendicular to the axis. The Poisson's ratio is set to 0.4995 for non-compressible biological material.

4.3 Results

The result is shown in Figure 8. The symbols denote experimental data and lines denote fits obtained from simulations. The experimental data are nominal stresses plotted against the stretch ratio when the transverse stretch ratio is 1.00. The experimental data shows the average of the 6 specimen test results. Experimental data in the x direction were used to acquire material constants and the prestresses, and then these values were then used to predict the corresponding responses in the y direction. The parameters (n , N and the prestresses) used in the simulation were determined by trial and error, fitting the predictions to the experimental data according to visual inspection (Birchoff, Arruda, & Grosh 2000). Good fit is found to the biaxial data.

The parameter obtained from the simulations are: collagen density $n = 3.0 \times 10^{24}/m^3$, the free length of the collagen fibers $N = 1.21$, prestress in x direction $\sigma_x = 38kPa$ and prestress in y direction $\sigma_y = 54kPa$.

Comparing the parameters obtained in this study with the parameters from Bischoff et al.'s (Birchoff, Arruda, & Grosh 2000) results, the network density n and prestresses are several orders less than Bischoff et al.'s results from *in vitro* uniaxial tests of rat dorsal skin, but is comparable to the parameters obtained from the *in vivo* uniaxial tests of human skin. One reason for the difference is that the rat dorsal skin does have bigger collagen density than the skin from abdominal area. Another reason may lie in that for the *in vivo* uniaxial test, the direction perpendicular to the stretching direction is not stress-free as in the *in vitro* test and it is more similar to the biaxial testing.

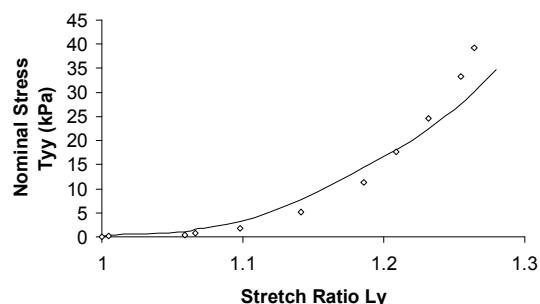
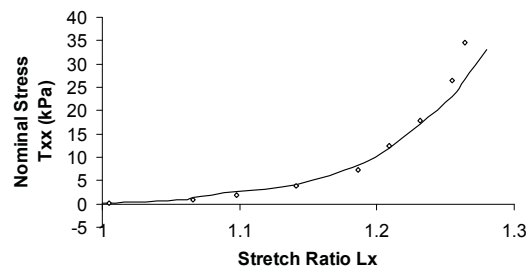


Figure 8: *In Vitro* biaxial test results and best-fit curves from finite element simulations.

5 Discussions

In this study, dynamic biaxial tests were performed on 16 pieces of abdominal skin specimen from rats. Based on the biaxial test results of skin, an isotropic structure constitutive model was used to model the anisotropic, non-linear properties of skin. By applying different prestresses at two orthogonal directions of skin, the model can predict the skin's non-linear and anisotropic properties.

To further build a more robust skin deformation model, there are some problems that need to be considered. First, shearing was ignored in the biaxial experiments in this study. The current extension testing alone could not provide sufficient information for a more applicable and accurate modeling of the skin deformation. So new measuring techniques for shearing and the *in vivo* collagen fiber density and orientation measurements should be applied in the future research. This will also help to build a physiological meaningful anisotropic, nonlinear constitutive model for biological soft tissues. Another thing need to be considered is that to simulate the *in vivo* behaviors

of skin more accurately for surgical applications, the special *in vivo* skin behaviors, which may involve the curve of the skin flaps and the behavior of the surrounding tissues, need to be studied and applied in the modeling of skin.

References

1. ABAQUS Inc. (2004). ABAQUS / CAE user's manual, V 6.4, ABAQUS Inc., Pawtucket, RI.
2. Alexander, H., & Cook, T. H. (1977). Accounting for the natural tension in the mechanical tension of human skin. *J Invest Dermatol* vol. 69, 310-314.
3. Arruda, E. M. & Boyce, M. C. (1993). A three-dimensional constitutive model for the large stretch behavior of rubber elastic materials. *J Mech Phys Solids* vol. 41, 389-412.
4. Berkley, J., Weghorst, S., Gladstone, H., Raugi, G., Berg, D., & Ganter, M. (1999) Fast finite element modeling for surgical simulation. *Stud Health Technol Inform* vol. 62, 55-61.
5. Bischoff, J.E., Arruda, E.M., & Grosh, K. (2000) Finite element modeling of human skin using an isotropic, nonlinear elastic constitutive model. *J Biomech* vol. 33, 645-652.
6. Bischoff, J.E., Arruda, E.M., & Grosh, K. (2004) A rheological network model for the continuum anisotropic and viscoelastic behavior of soft tissue. *Biomech Model Mechanobiol* vol. 3, 56-65.
7. Clark, J.A., Cheng, J.C., & Leung, K.S. (1996) Mechanical properties of normal skin and hypertrophic scars. *Burns* vol. 22, 443-446.
8. Dehoff, P. H., & Key, J. E. (1981). Application of the finite element analysis to determine forces and stresses in wound closing. *J Biomech* vol. 14, 549-554.
9. Demiray, H., & Vito, R. P. (1976). Large deformation analysis of soft biomaterials, *Int J Eng Sci* vol. 14, 789-793.
10. Flynn, D. M., Peura, G. D., Grigg, P., & Hoffman, A. H. (1998). A finite element based method to determine the properties of planar soft tissue. *J Biomech Eng* vol. 120, 202-210.
11. Fung, Y. C. (1993). Biomechanics: Mechanical Properties of Living Tissues. 2nd edition, Springer-Verlag, New York, pp. 293-311.
12. Gambarotta, L., Massabo, R., Morbiducci, R., Raposio, E., & Santi, P. (2005). In vivo experimental testing and model identification of human scalp skin. *J Biomech* vol. 38, 2237-2247.
13. Gao, J., Huang, W., & Yen, M. Y. C. (1998). Strip biaxial experiments of human parenchyma. *Adv Bioeng* vol. 39, 241-242.
14. Gibson, T., Stark, H., & Evans, J. H. (1969). Directional variation in the extensibility of human skin in vivo. *J Biomech* vol. 2, 201-204.
15. Grahame, R. (1969). Elasticity of human skin in vivo, a study of the physical properties of the skin in rheumatoid arthritis and the effect of corticosteroids. *Ann phys Med* vol. 10, 130-136.
16. Hendriks, F. M., Brokken, D., Van Eemeren, J. T., Oomens, C. W., Baaijens, F. P., & Horsten, J. B. (2003). A numerical-experimental method to characterize the nonlinear mechanical behaviour of human skin. *Skin Res Technol* vol. 9, 274-283.
17. Hildebrandt, J., Fukaya, H., & Martin, C. J. (1969). Simple uniaxial and uniform biaxial deformation of nearly isotropic incompressible tissues. *Biophys J* vol. 9, 781-791.
18. Holberg, C., Schwenzer, K., & Rudzki-Janson, I. (2005). Three-dimensional soft tissue prediction using finite elements. Part I: Implementation of a new procedure. *J Orofac Orthop* vol. 66, 110-121.
19. Holberg, C., Heine, A. K., Geis, P., Schwenzer, K., & Rudzki-Janson, I. (2005). Three-dimensional soft tissue prediction using finite elements. Part II: Clinical application. *J Orofac Orthop* vol. 66, 122-134.

20. Kirby, S. D., Wang, B., To, C. W., & Lampe, H. B. (1998). Nonlinear, three-dimensional finite-element model of skin biomechanics. *J Otolaryngol* vol. 27, 153-160.
21. Kirk, E., & Chieffi, M. (1962). Variation with age in elasticity of skin and subcutaneous tissue in human individuals. *J Gerontol* vol. 17, 373-380.
22. Lanir, Y., & Fung, Y. C. (1974). Two-dimensional mechanical properties of rabbit skin. I. Experimental system. *J Biomech* vol. 7, 29-34.
23. Lanir, Y., & Fung, Y. C. (1974). Two-dimensional mechanical properties of rabbit skin. II. Experimental results. *J Biomech* vol. 7, 171-182.
24. Lanir, Y. (1994). Plausibility of structural constitutive equations for isotropic soft tissues in finite static deformations. *J App Mech* vol. 61, 695-702.
25. Larrabee, W. F., Jr. (1986). A finite element model of skin deformation. I. Biomechanics of skin and soft tissue: a review. *Laryngoscope* vol. 96, 399-405.
26. Larrabee, W. F., Jr., & Sutton, D. (1986). A finite element model of skin deformation. II. An experimental model of skin deformation. *Laryngoscope* vol. 96, 406-412.
27. Larrabee, W. F., Jr., & Galt, J. A. (1986). A finite element model of skin deformation. III. The finite element model. *Laryngoscope* vol. 96, 413-419.
28. Lott-Crumpler, D. A., & Chaudhry, H. R. (2001). Optimal patterns for suturing wounds of complex shapes to foster healing. *J Biomech* vol. 34, 51-58.
29. Molinari, E., Fato, M., De Leo, G., Riccardo, D., & Beltrame, F. (2005). Simulation of the biomechanical behavior of the skin in virtual surgical applications by finite element method. *IEEE Trans Biomed Eng* vol. 52, 1514-1521.
30. Nielsen, P. M. F., Hunter, P. J., & Smaill, B. H. (1991). Biaxial testing of membrane biomaterials: testing equipment and procedures. *J Biomech Eng* vol. 113, 295-300.
31. Ohura, T., Singihara, T. & Honda, K. (1980). Postoperative evaluation in plastic surgery using the bio-skin tension meter. *Ann Plastic Surg* vol. 5, 74-82.
32. Retel, V., Vescovo, P., Jacquet, E., Trivaudey, F., Varchon, D., & Burtheret, A. (2001). Non-linear model of skin mechanical behaviour analysis with finite element method. *Skin Res Technol* vol. 7, 152-158.
33. Ridge, M. D., & Wright, V. (1966). Mechanical properties of skin. A bioengineering study of skin structure. *J App Phys* vol. 21, 1602-1606.
34. Sacks, M. S. (2000). Biaxial Mechanical Evaluation of Planar Biological Materials, *J Elasticity* vol. 61, 199-246.
35. Sacks, M. S., & Sun, W. (2003). Multiaxial mechanical behavior of biological materials. *Ann Rev Biomed Eng* vol. 5, 251-284.
36. Schneider, D. C., Davidson, T. M. & Nahum, N. A. (1984). In vitro biaxial stress strain response of human skin. *Arch Otolaryngol* vol. 110, 329-333.
37. Shoemaker, P. A., Schneider, D., Lee, M. C., & Fung, Y. C. (1986). A constitutive model for two-dimensional soft tissues and its application to experimental data. *J Biomech* vol. 19, 695-702.
38. Spilker, R. L., de Almeida, E. S., & Donzelli, P. S. (1992). Finite element methods for the biomechanics of soft hydrated tissues: nonlinear analysis and adaptive control of meshes. *Crit Rev Biomed Eng* vol. 20, 279-313.
39. Thacker, J. G., Lachetta, F. A., Allaire, P. E., Edgerton, M. T., Rodeheaver, G. T. & Edlich, R. F. (1977). In Vivo extensometer for measurement of the biomechanical properties of human skin. *Rev Sci Instrum* vol. 48, 181-185.

40. Tong, P., & Fung, Y. C. (1976). The stress-strain relationship for the skin. *J Biomech* vol. 9, 649-657.
41. Wan Abas, W. A. (1994). Biaxial tension test of human skin in vivo. *Biomed Mater Eng* vol. 4, 473-486.
42. Wilkes, G. L., Brown, I. A., & Wildnauer, R. H. (1973). The biomechanical properties of skin. *CRC Crit Rev Bioeng* vol. 1, 453-495.
43. Yoshida, H., Tsutsumi, S., Mizunuma, M., & Yanai, A. (2001). A surgical simulation system of skin sutures using a three-dimensional finite element method. *Clin Biomech (Bristol, Avon)* vol. 16, 621-626.